British Journal of Pharmacology (2009), 156, 587–600

0007-1188/09
www.brjpharmacol.org

RESEARCH PAPER

Mechanism of asynchronous Ca^{2+} waves underlying agonist-induced contraction in the rat basilar artery

HT Syyong[1,2], HHC Yang[1,2], G Trinh[2], C Cheung[2], KH Kuo[1] and C van Breemen[1,2]

[1]*Department of Anesthesiology, Pharmacology & Therapeutics, University of British Columbia, Vancouver, British Columbia, Canada, and* [2]*Cardiovascular Sciences, Child and Family Research Institute; University of British Columbia, Vancouver, British Columbia, Canada*

Background and purpose: Uridine 5′-triphosphate (UTP) is a potent vasoconstrictor of cerebral arteries and induces Ca^{2+} waves in vascular smooth muscle cells (VSMCs). This study aimed to determine the mechanisms underlying UTP-induced Ca^{2+} waves in VSMCs of the rat basilar artery.
Experimental approach: Isometric force and intracellular Ca^{2+} ($[Ca^{2+}]_i$) were measured in endothelium-denuded rat basilar artery using wire myography and confocal microscopy respectively.
Key results: Uridine 5′-triphosphate (0.1–1000 $\mu mol \cdot L^{-1}$) concentration-dependently induced tonic contraction ($pEC_{50} = 4.34 \pm 0.13$), associated with sustained repetitive oscillations in $[Ca^{2+}]_i$ propagating along the length of the VSMCs as asynchronized Ca^{2+} waves. Inhibition of Ca^{2+} reuptake in sarcoplasmic reticulum (SR) by cyclopiazonic acid abolished the Ca^{2+} waves and resulted in a dramatic drop in tonic contraction. Nifedipine reduced the frequency of Ca^{2+} waves by 40% and tonic contraction by 52%, and the nifedipine-insensitive component was abolished by SKF-96365, an inhibitor of receptor- and store-operated channels, and KB-R7943, an inhibitor of reverse-mode Na^+/Ca^{2+} exchange. Ongoing Ca^{2+} waves and tonic contraction were also abolished after blockade of inositol-1,4,5-triphosphate-sensitive receptors by 2-aminoethoxydiphenylborate, but not by high concentrations of ryanodine or tetracaine. However, depletion of ryanodine-sensitive SR Ca^{2+} stores prior to UTP stimulation prevented Ca^{2+} waves.
Conclusions and implications: Uridine 5′-triphosphate-induced Ca^{2+} waves may underlie tonic contraction and appear to be produced by repetitive cycles of regenerative Ca^{2+} release from the SR through inositol-1,4,5-triphosphate-sensitive receptors. Maintenance of Ca^{2+} waves requires SR Ca^{2+} reuptake from Ca^{2+} entry across the plasma membrane via L-type Ca^{2+} channels, receptor- and store-operated channels, and reverse-mode Na^+/Ca^{2+} exchange.
British Journal of Pharmacology (2009) **156**, 587–600; doi:10.1111/j.1476-5381.2008.00063.x; published online 19 January 2009

Keywords: calcium oscillations; calcium waves; basilar artery; vascular smooth muscle; confocal microscopy; uridine 5′-triphosphate

Abbreviations: $[Ca^{2+}]_i$, intracellular Ca^{2+}; 2-APB, 2-aminoethoxydiphenylborate; CPA, cyclopiazonic acid; $Ins(1,4,5)P_3$, inositol 1,4,5-trisphosphate; IP_3R, inositol-1,4,5-triphosphate receptor; RyR, ryanodine receptor; SR, sarcoplasmic reticulum; UTP, uridine 5′-triphosphate; VSMCs, vascular smooth muscle cells

Introduction

Uridine 5′-triphosphate (UTP) is a potent constrictor of cerebral arteries which exerts its effects through purinergic P2Y receptors and the phospholipase C pathway (Urquilla, 1978; Strobaek *et al.*, 1996; Horiuchi *et al.*, 2001). Brain tissue is especially rich in UTP and cerebral vessels have greater reactivity to UTP compared with other vessels (Shirasawa *et al.*, 1983; Hardebo *et al.*, 1987). UTP may be involved in the regulation of cerebrovascular tone under both physiological conditions and pathophysiological reactions in disease states such as subarachnoid haemorrhage or migraine (Debdi *et al.*, 1992; Boarder and Hourani, 1998; Burnstock, 1998).

Smooth muscle contraction is initiated by an increase of intracellular Ca^{2+} ($[Ca^{2+}]_i$) from resting levels of ~100 $nmol \cdot L^{-1}$ to values up to 1 $\mu mol \cdot L^{-1}$. In general, the $[Ca^{2+}]_i$ profile following stimulation is biphasic, consisting of a rapid transient rise in $[Ca^{2+}]_i$ from sarcoplasmic reticulum (SR) Ca^{2+} release followed by a plateau phase, which is mediated by Ca^{2+} entry from voltage-gated Ca^{2+} channels and store/receptor-operated channels (van Breemen *et al.*, 1978; Bolton, 1979; Streb *et al.*, 1983; Putney, 1986). The advent of confocal microscopy has

Correspondence: Dr C van Breemen, Cardiovascular Sciences, Child and Family Research Institute, Room 2099 – 950 W 28th Avenue, Vancouver, British Columbia, Canada, V5Z 4H4. E-mail: breemen@interchange.ubc.ca
Received 6 August 2008; accepted 2 October 2008

allowed the employment of physiological preparations to examine the Ca^{2+} signals in individual *in situ* vascular smooth muscle cells (VSMCs) of intact blood vessels. It has since become apparent that the average arterial wall $[Ca^{2+}]_i$ observed previously is not representative of the Ca^{2+} signalling events within individual VSMCs, which are capable of generating Ca^{2+} signals with varying spatial and temporal patterns (see Lee *et al.*, 2002). Among these signals are Ca^{2+} waves, which are manifested as changes in $[Ca^{2+}]_i$ which travel the length of VSMCs, and constitute a specialized form of agonist-induced Ca^{2+} signalling which appears to be involved in contractile regulation. Since 1994 when they were first described, Ca^{2+} waves have been observed in the smooth muscle fibres of a variety of intact blood vessels, including cerebral vessels (Iino *et al.*, 1994; Asada *et al.*, 1999; Miriel *et al.*, 1999; Jaggar, 2001; Lee *et al.*, 2001; Peng *et al.*, 2001). Although there are likely to be underlying physiological reasons for signalling with Ca^{2+} waves (as opposed to steady state $[Ca^{2+}]_i$ elevations), the mechanisms behind how Ca^{2+} waves within individual VSMCs signal for contraction remain poorly understood.

Ca^{2+} waves in cerebral arteries can be induced by a variety of stimuli, including vasoconstrictor agonists such as UTP, pressure and alkaline pH (Jaggar and Nelson, 2000; Jaggar, 2001; Heppner *et al.*, 2002). In cerebral arteries, UTP stimulation shifts Ca^{2+} sparks to Ca^{2+} waves through the differential regulation of inositol-1,4,5-triphosphate receptors (IP_3Rs) and ryanodine receptors (RyRs) (Jaggar and Nelson, 2000). From studies in cultured basilar artery smooth muscle cells, it is generally accepted that UTP induces vasoconstriction by a combination of stimulated plasma membrane Ca^{2+} entry and SR Ca^{2+} release (Sima *et al.*, 1997). However, little is known about the mechanism underlying between agonist-induced Ca^{2+} waves and their relationship to vasoconstriction in the cerebral vasculature.

In our present study, we investigated the mechanism of UTP-induced Ca^{2+} waves in the rat basilar artery, focusing on the mode(s) of Ca^{2+} entry involved in sustaining the UTP-induced cyclical release of Ca^{2+} by identifying the Ca^{2+} transport molecules involved in the generation and maintenance of UTP-induced Ca^{2+} waves.

Methods

Experimental animals and tissue preparation

All animal experiments and procedures were carried out in accordance with the guidelines of the University of British Columbia. Male Sprague-Dawley rats (250–350 g) were obtained from Charles River and housed in the institutional animal facility (University of British Columbia, Child and Family Research Institute) under standard animal room conditions (12 h light–12 h dark, at 25°C, two animals in a cage). Rats were anesthetized with a mixture of ketamine hydrochloride (70 $mg \cdot kg^{-1}$) and xylazine hydrochloride (5 $mg \cdot kg^{-1}$) given intraperitoneally. The brain was quickly removed and placed in ice-cold, oxygenated (95% O_2–5% CO_2) Krebs solution. The basilar artery (180–280 μm in diameter) was removed, carefully cleaned and cut into 2 mm segments. Endothelial denudation was achieved by gently rubbing the inside of the vessel with a 40 μm tungsten wire.

Measurement of $[Ca^{2+}]_i$

The arterial rings were loaded with Fluo-4AM (5 $\mu mol \cdot L^{-1}$ with 5 $\mu mol \cdot L^{-1}$ Pluronic F-127, 1 h at 37°C) and isometrically mounted, followed by a 30 min washout time in HEPES-buffered physiological saline solution (PSS). Sustained Ca^{2+} waves were induced by 100 $\mu mol \cdot L^{-1}$ UTP, and all mechanistic studies were carried out at this concentration. Images were acquired on an upright Olympus BX50WI microscope with a 60× water-dipping objective (NA 0.9) and equipped with an Ultraview confocal imaging system (Perkin-Elmer). The tissue was illuminated using the 488 nm line of an Argon-Krypton laser and a high-gain photomultiplier tube collected the emission at wavelengths between 505 and 550 nm. The scanned regions correspond to a 91.685 × 66.68 μm area (or 248 × 328 pixels). The representative fluorescence traces shown reflect the averaged fluorescence signals from a region of 3 × 3 pixels (1.69 μm^2) of the VSMC. The rate of image acquisition was three $frames \cdot s^{-1}$. The frequency of Ca^{2+} waves was determined by counting the number of waves occurring within 40 s. The measured changes in Fluo-4 fluorescence level are proportional to the relative changes in $[Ca^{2+}]_i$. All parameters (laser intensity, gain, etc.) were maintained constant during the experiment. The confocal images were analysed off-line with the Ultraview 4.0 Software (Perkin-Elmer). Fluorescence traces were extracted from the movies to exclude nuclear regions and traces were normalized to initial fluorescence values.

Measurement of isometric force

Basilar artery segments were mounted isometrically in a small vessel wire myograph (A/S Danish Myotechnology, Aarhus N, Denmark) using two 40 μm tungsten wires, for measuring generated force. The chambers were kept at 37°C and bubbled continuously with 95% O_2–5% CO_2 in Krebs solution. Optimal tension (3 mN) was determined in preliminary experiments by subjecting arterial segments to different resting tensions and stimulating with 60 $mmol \cdot L^{-1}$ KCl. The vessels were stretched to the optimal tension for 60 min and challenged twice with 60 $mmol \cdot L^{-1}$ KCl before experiments were continued. The percent of contraction compared with the second 60 $mmol \cdot L^{-1}$ KCl-induced contraction was recorded at different concentrations of UTP and concentration-response curves were constructed. Tonic contraction was induced by 100 $\mu mol \cdot L^{-1}$ UTP and all mechanistic studies carried out at this concentration. The negative logarithm (pD_2) of the concentration of UTP giving half-maximum response (EC_{50}) was assessed by linear interpolation on the semilogarithm concentration-response curve [$pD_2 = -\log(EC_{50})$].

Statistics

Values are expressed as mean ± standard error (SE) from at least six independent experiments. Statistical analysis and construction of concentration-response curves were performed using GraphPad Prism 4.0 software (San Diego, CA, USA). Differences between groups were analysed by Student's two-tailed *t*-test. Statistical significance was defined as P values <0.05.

Drugs, solutions and chemicals

HEPES-PSS containing (in $mmol \cdot L^{-1}$) NaCl 140, glucose 10, KCl 5, HEPES 5, $CaCl_2$ 1.5 and $MgCl_2$ 1 (pH 7.4) was used for

all confocal studies. High-K^+ (60 mmol·L^{-1} extracellular K^+) PSS was identical in composition to normal PSS with the exception of (in mmol·L^{-1}) NaCl 85 and KCl 60. Zero-Ca^{2+} PSS was prepared in the same way as normal PSS, but $CaCl_2$ was replaced with 1 mmol·L^{-1} EGTA. Krebs solution containing (in mmol·L^{-1}) NaCl 119, glucose 11.1, KCl 4.7, $CaCl_2$ 1.6, KH_2PO_4 1.18, $MgSO_4$ 1.17 and EDTA 0.023 (pH 7.4) was used for all isometric contraction studies.

Uridine 5′-triphosphate, cyclopiazonic acid (CPA), 2-aminoethoxydiphenylborate (2-APB), nifedipine, SKF-96365, tetracaine and pluronic F-127 were obtained from Sigma-Aldrich (Oakville, Ontario, Canada). Ryanodine and KB-R7943 were obtained from Calbiochem (Gibbstown, NJ, USA). Fluo-4AM was purchased from Molecular Probes (Eugene, OR, USA). All drug and molecular target nomenclature conforms to the British Journal of Pharmacology's Guide to Receptors and Channels (Alexander *et al.*, 2008).

Results

Relation between UTP-induced tonic contraction and UTP-induced Ca^{2+} waves

Uridine 5′-triphosphate produced tonic contraction in a concentration-dependent manner, with a pEC_{50} of 4.34 ± 0.13 and maximal response (E_{max}) of 105.5 ± 7.3% ($n = 9$ animals, Figure 1A,B). At 100 μmol·L^{-1} UTP, the average contraction was 70.3 ± 4.5% ($n = 12$ animals, normalized to 60 mmol·L^{-1} KCl). In parallel experiments, confocal microscopy was used to observe changes in $[Ca^{2+}]_i$ within the VSMCs following UTP stimulation. In the absence of UTP, asynchronous Ca^{2+} waves of low amplitude were observed in a small percentage (<10%) of the cells, similar to the 'Ca^{2+} ripples' described previously in rat tail artery (Asada *et al.*, 1999). Application of UTP induced a large transient Ca^{2+} response

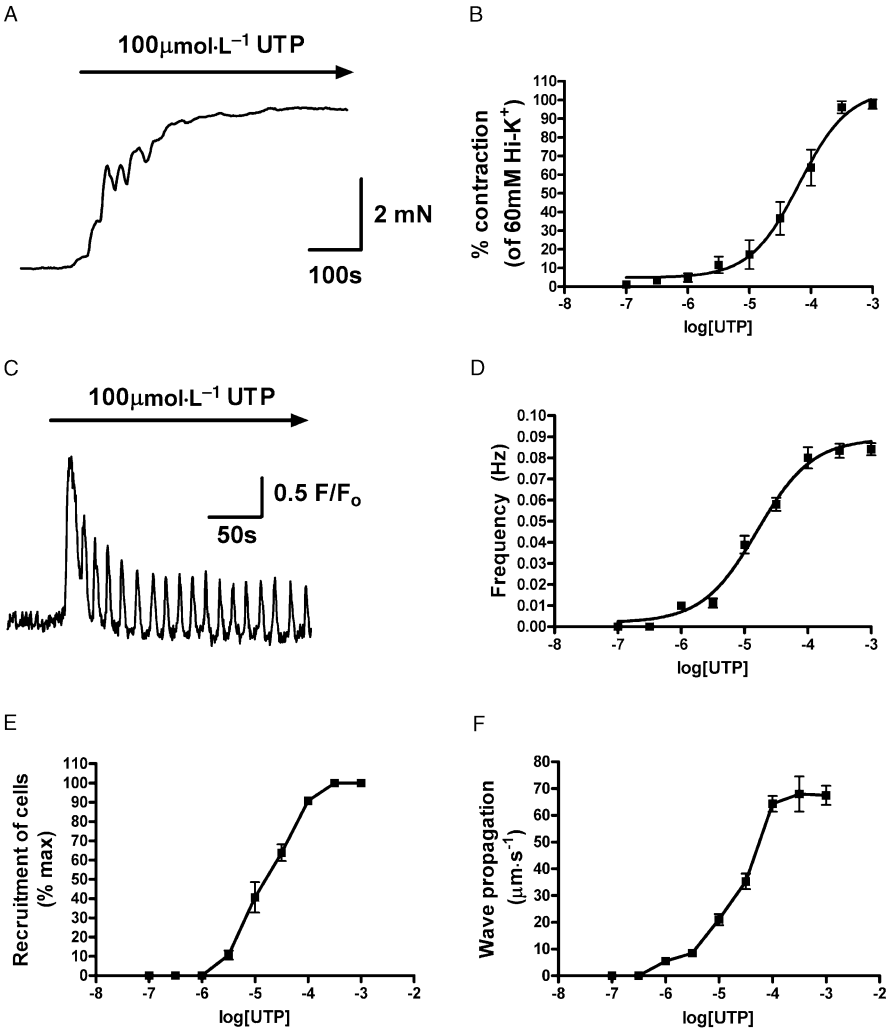

Figure 1 Properties of uridine 5′-triphosphate (UTP)-induced Ca^{2+} waves underlying tonic contraction in rat basilar artery. (A) UTP (100 μmol·L^{-1})-induced tonic contraction. Traces are representative of results from six animals. (B) Concentration-response curve for UTP-induced tonic contraction. $pEC_{50} = 4.24 \pm 0.13$ ($n = 9$ animals) (C) In parallel experiments, application of UTP (100 μmol·L^{-1}) produced sustained Ca^{2+} oscillations. Experimental Ca^{2+} traces are representative of results from 58 cells from six animals. (D) Concentration-response curve for frequency of UTP-induced Ca^{2+} waves $pEC_{50} = 4.74 \pm 0.14$ ($n = 109$ cells from 12 animals). (E) A greater percentage of VSMCs generated Ca^{2+} signals as UTP concentration increased. This recruitment occurred between 3 and 1000 μmol·L^{-1}, with maximal recruitment achieved at 300 μmol·L^{-1} UTP ($n = 90$ cells from 10 animals). The number of cells firing is expressed as a percentage of cells responding to maximal concentration. (F) The apparent propagation speed of the Ca^{2+} waves was correlated to increasing UTP concentration ($n = 87$ cells from 11 animals).

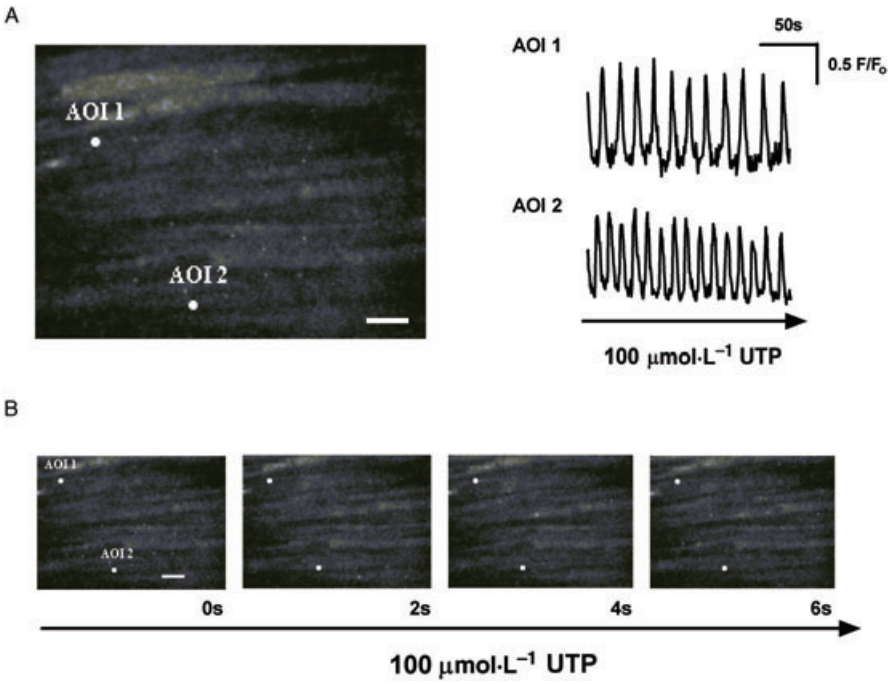

Figure 2 Uridine 5′-triphosphate (UTP)-induced Ca^{2+} waves in rat basilar artery. (A) $[Ca^{2+}]_i$ changes in two intracellular regions from two different smooth muscle cells upon UTP (100 μmol·L^{-1}) stimulation are depicted in the Ca^{2+} traces taken from the steady state of UTP-induced Ca^{2+} waves. It should be noted that the Ca^{2+} waves occurred at different frequencies. Experimental Ca^{2+} traces are representative of results from 58 cells in six animals. (B) Intact rat basilar artery smooth muscle cells challenged with UTP (100 μmol·L^{-1}) displayed Ca^{2+} waves which originated from distinct intracellular foci and propagated along the longitudinal axis of the smooth muscle cells (indicated by AOI1 and AOI2). The area of AOI is 3 × 3 pixels (1.69 μm^2). Scale bar = 10 μm.

which was followed by sustained repetitive oscillations in intracellular $[Ca^{2+}]_i$ which propagated along the length of the VSMC as Ca^{2+} waves (Figures 1C and 2). The frequency of Ca^{2+} waves increased in a concentration-dependent manner, closely paralleling the development of force (Figure 1D, pEC_{50} = 4.74 ± 0.14, maximum frequency = 0.089 ± 0.007 Hz, 109 cells from 12 animals). At 100 μmol·L^{-1} UTP, the average frequency of the Ca^{2+} waves was 0.082 ± 0.005 Hz (n = 48 cells from eight animals). The number of cells displaying Ca^{2+} waves was also concentration-dependent; at 100 μmol·L^{-1} UTP, 91 ± 2.5% of cells displayed at least one Ca^{2+} wave (n = 48 cells from eight animals, Figure 1E). The velocity of wave propagation, illustrated in Figure 1F, also shows a strong dependence on concentration of UTP. At the highest concentrations, wave propagation speeds reached 67.5 ± 3.6 μm·s^{-1} (n = 10 cells from four animals). The Ca^{2+} waves originated from distinct intracellular foci and propagated down the longitudinal axis of the individual VSMCs (Figure 2). They did not appear to propagate intercellularly, and were sustained during the entire experimental period.

Dependence of UTP-induced Ca^{2+} waves on extracellular Ca^{2+} influx

There are two potential sources of Ca^{2+} that can contribute to the generation of UTP-induced Ca^{2+} waves: Ca^{2+} release from the intracellular stores and Ca^{2+} influx from the extracellular space. To determine the contribution of extracellular Ca^{2+} to the initiation and maintenance of UTP-induced Ca^{2+} waves, extracellular Ca^{2+} was removed prior to and during 100 μmol·L^{-1} UTP stimulation respectively. Removal of extracellular Ca^{2+} immediately prior to UTP stimulation reduced the Ca^{2+} signal to only a few transient Ca^{2+} waves (n = 39 cells from six animals, Figure 3A), while UTP-induced Ca^{2+} waves were completely abolished in the absence of extracellular Ca^{2+} within 1 min of treatment (n = 34 cells from five animals) (Figure 3B), showing that extracellular Ca^{2+} influx was necessary for maintenance of Ca^{2+} waves.

To further define the Ca^{2+} entry pathways involved in maintaining UTP-induced Ca^{2+} waves, nifedipine, a selective inhibitor of L-type Ca^{2+} channels, and SKF-96365, an inhibitor of receptor- and store-operated channels, were used. Nifedipine (10 μmol·L^{-1}) reduced the frequency of 100 μmol·L^{-1} UTP-induced Ca^{2+} waves to 59 ± 4% of control, while the combined application of nifedipine and SKF-96365 (50 μmol·L^{-1}) completely abolished the Ca^{2+} waves (P < 0.001, n = 42 cells from eight animals). In parallel, application of nifedipine (10 μmol·L^{-1}) significantly reduced tonic contraction to 52 ± 4% of control (P < 0.001, n = 6 animals), while the additional application of SKF-96365 (50 μmol·L^{-1}) decreased tonic contraction to 2.2 ± 1.1% of control (P < 0.001, n = 5 animals) (Figure 4A,B). It should also be noted that nifedipine (10 μmol·L^{-1}) completely abolished the contraction induced by 60 mmol·L^{-1} KCl (data not shown).

In addition to the conventional plasmalemmal Ca^{2+} permeable channels, the Na^+/Ca^{2+} exchanger operating in the reverse-mode is also an important pathway for Ca^{2+} entry in VSMCs (Lee *et al.*, 2002; Poburko *et al.*, 2006; Fameli *et al.*, 2007). KB-R7943, an inhibitor of reverse-mode Na^+/Ca^{2+} exchange at low (≤10 μmol·L^{-1}) concentrations, was used to examine

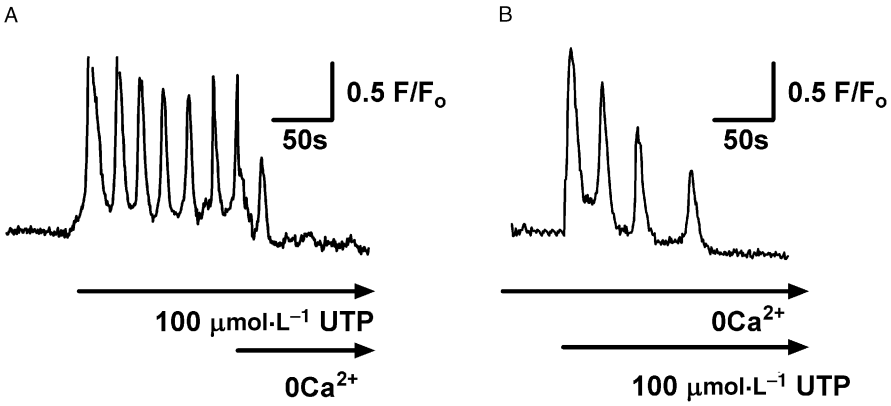

Figure 3 Extracellular Ca^{2+} influx is required for maintenance of uridine 5′-triphosphate (UTP)-induced Ca^{2+} waves. (A) Removal of extracellular Ca^{2+} during ongoing UTP (100 μmol·L^{-1})-induced Ca^{2+} waves results in their disappearance within 1 min. Traces shown are representative of 39 cells from six animals. (B) Removal of extracellular Ca^{2+} immediately prior to UTP (100 μmol·L^{-1}) stimulation limits Ca^{2+} signalling to transient Ca^{2+} waves. Traces shown are representative of 34 cells from five animals.

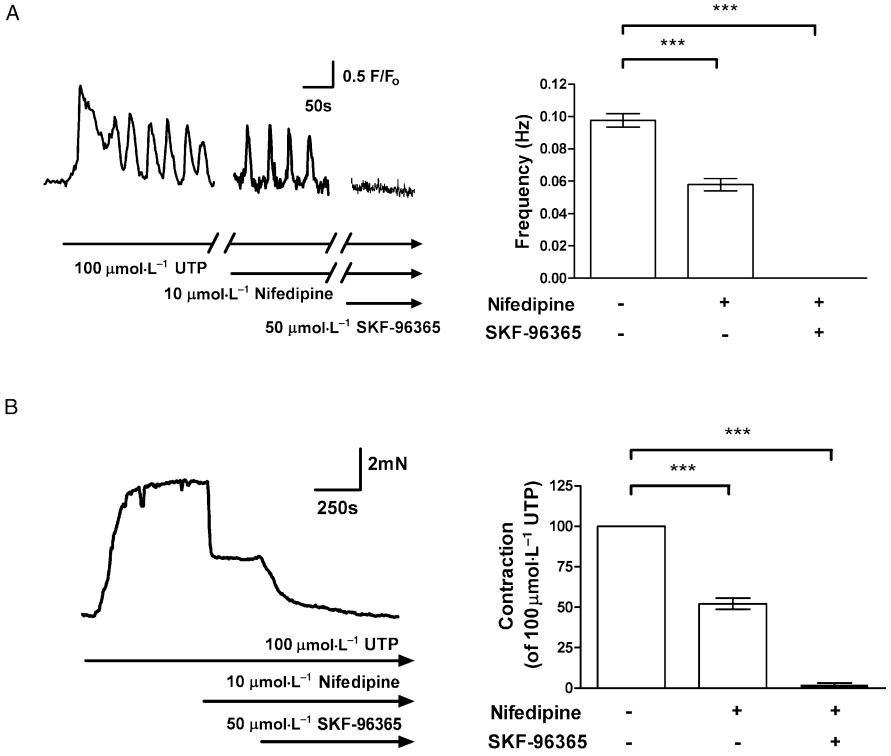

Figure 4 Effect of L-type Ca^{2+} channel antagonist nifedipine and receptor/store-operated channel antagonist SKF-96365 on uridine 5′-triphosphate (UTP) (100 μmol·L^{-1})-induced Ca^{2+} waves and tonic contraction. (A) The frequency of Ca^{2+} waves is significantly reduced following nifedipine (10 μmol·L^{-1}) application, but not abolished. The nifedipine-insensitive component is completely abolished following addition of SKF-96365 (50 μmol·L^{-1}). The breaks in the record indicate a 2 min interval. (B) UTP (100 μmol·L^{-1})-induced tonic contraction is significantly reduced by nifedipine (10 μmol·L^{-1}) and almost completely abolished after SKF-96365 (50 μmol·L^{-1}). ***$P < 0.001$.

whether reverse-mode Na^+/Ca^{2+} exchange is involved in supporting nifedipine-insensitive Ca^{2+} waves (Iwamoto *et al.*, 1996; Ladilov *et al.*, 1999). The application of KB-R7943 (10 μmol·L^{-1}) abolished nifedipine-insensitive Ca^{2+} waves ($P < 0.001$, $n = 34$ cells from six animals) and inhibited tonic contraction to 3.6 ± 1.0% of control ($P < 0.001$, $n = 7$ animals) (Figure 5A,B). Application of KB-R7943 (10 μmol·L^{-1}) by itself also abolished UTP-induced Ca^{2+} waves ($P < 0.001$, $n = 29$ cells from four animals) and tonic contraction ($P < 0.001$, $n = 4$ animals), suggesting that Ca^{2+} entry through reverse-mode Na^+/Ca^{2+} exchange plays an important role in maintenance of Ca^{2+} waves even when L-type Ca^{2+} channels are operative (Figure 5C,D). Although KB-R7943 (10 μmol·L^{-1}) reduced 60 mmol·L^{-1} KCl-induced tonic contraction by 10.6% ± 3.0%, this effect was not significant ($P = 0.08$, $n = 5$ animals) (Figure 6A). KB-R7943 may also inhibit store-operated channels (Arakawa *et al.*, 2000). To test for possible effects on store-operated channels, we used UTP (100 μmol·L^{-1}) to stimulate sustained Ca^{2+} waves and then applied CPA (10 μmol·L^{-1}), an inhibitor of the sarco(endo)plasmic reticulum Ca^{2+}-ATPase,

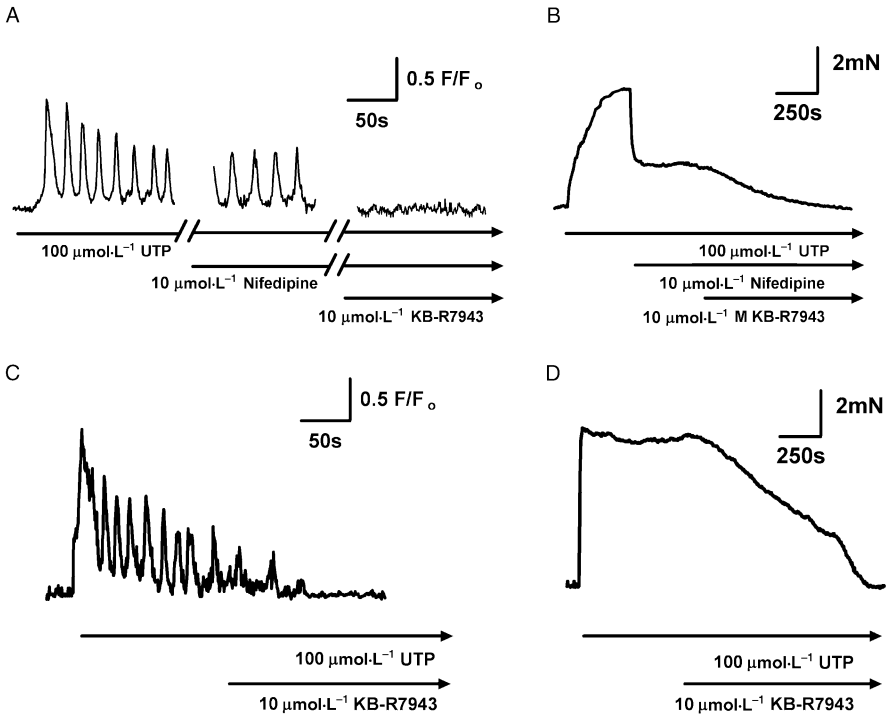

Figure 5 Effect of the reverse-mode Na^+/Ca^{2+} exchanger inhibitor KB-R7943 on uridine 5′-triphosphate (UTP)-induced Ca^{2+} waves and tonic contraction. (A) Blockade of reverse (Ca^{2+}-entry) mode Na^+/Ca^{2+} exchange using KB-R7943 (10 μmol·L^{-1}) abolished the nifedipine-resistant UTP (100 μmol·L^{-1})-induced Ca^{2+} waves ($P < 0.001$, $n = 34$ cells from six animals) (B) Similarly, KB-R7943 (10 μmol·L^{-1}) also inhibited the nifedipine-insensitive tonic contraction to 3.6 ± 1.0% of control ($P < 0.001$, $n = 6$ animals) (C) Application of KB-R7943 (10 μmol·L^{-1}) alone reduced the frequency of UTP (100 μmol·L^{-1})-induced Ca^{2+} waves, followed by complete abolition ($P < 0.001$, $n = 29$ cells from four animals) (D) KB-R7943 (10 μmol·L^{-1}) alone also abolished UTP (100 μmol·L^{-1})-induced tonic contraction ($P < 0.001$, $n = 5$ animals).

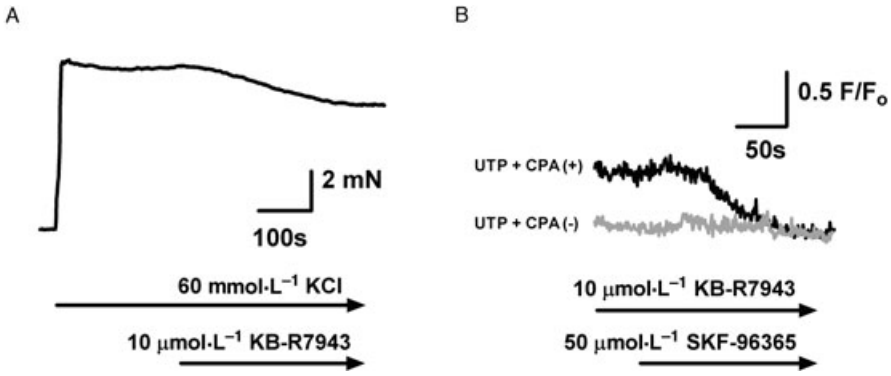

Figure 6 Effects of KB-R7943 on L-type Ca^{2+} channels and store/receptor-operated channels in rat basilar artery. (A) Application of KB-R7943 reduced tonic contraction induced by 60 mmol·L^{-1} KCl by 10.6 ± 3.0% ($P = 0.08$, $n = 5$ animals). (B) Application of uridine 5′-triphosphate (UTP) (100 μmol·L^{-1}) followed by cyclopiazonic acid (CPA) (10 μmol·L^{-1}) resulted in a maintained elevation in Ca^{2+}. Application of KB-R7943 (10 μmol·L^{-1}) did not affect this plateau response, whereas the addition of SKF-96365 (50 μmol·L^{-1}) abolished the maintained Ca^{2+} elevation and returned to pre-stimulation baseline level. Representative trace shown is typical of the responses obtained in 36 cells from four rats.

to inhibit SR Ca^{2+} reuptake. This resulted in an elevation of $[Ca^{2+}]_i$, on which KB-R7943 had no effect, although the addition of SKF-96365 brought $[Ca^{2+}]_i$ to baseline (Figure 6B). This suggests that KB-R7943 did not abolish the Ca^{2+} waves through blockade of store/receptor-operated channels. It is also important to note that extracellular Na^+-depletion with the use of zero-Na^+ PSS also abolished the Ca^{2+} waves, which further supports the role of reverse-mode Na^+/Ca^{2+} exchange (data not shown).

Dependence of UTP-induced Ca^{2+} waves on SR Ca^{2+} release

The all-or-none wave-like nature of Ca^{2+} signal in the rat basilar artery suggests regenerative Ca^{2+} release from the SR. If this is the case, blockade of SR Ca^{2+} uptake should completely inhibit the Ca^{2+} waves. The application of CPA (10 μmol·L^{-1}) to ongoing UTP-induced Ca^{2+} waves resulted in a broadening of the Ca^{2+} waves followed by their complete abolition, leaving a significant elevation in baseline $[Ca^{2+}]_i$ corresponding to 35 ± 4% of the peak $[Ca^{2+}]$ of the Ca^{2+} waves ($P < 0.001$,

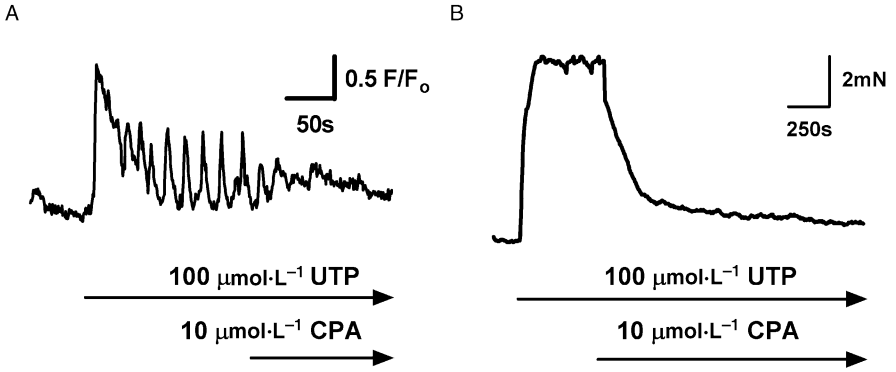

Figure 7 Effect of blockade of the sarco(endo)plasmic reticulum Ca^{2+} ATPase by cyclopiazonic acid (CPA) on uridine 5′-triphosphate (UTP)-induced Ca^{2+} waves. (A) Addition of CPA (10 μmol·L^{-1}) to ongoing UTP (100 μmol·L^{-1})-induced Ca^{2+} waves completely abolished the oscillations, leaving a small but significant elevation in baseline Ca^{2+} which corresponds to 35 ± 4% of the peak [Ca^{2+}] of the asynchronous Ca^{2+} waves ($P < 0.001$, $n = 28$ cells from five animals) (B) Application of CPA (10 μmol·L^{-1}) produced a 79 ± 2% inhibition of the UTP (100 μmol·L^{-1})-induced tonic contraction ($P < 0.001$, $n = 5$ animals).

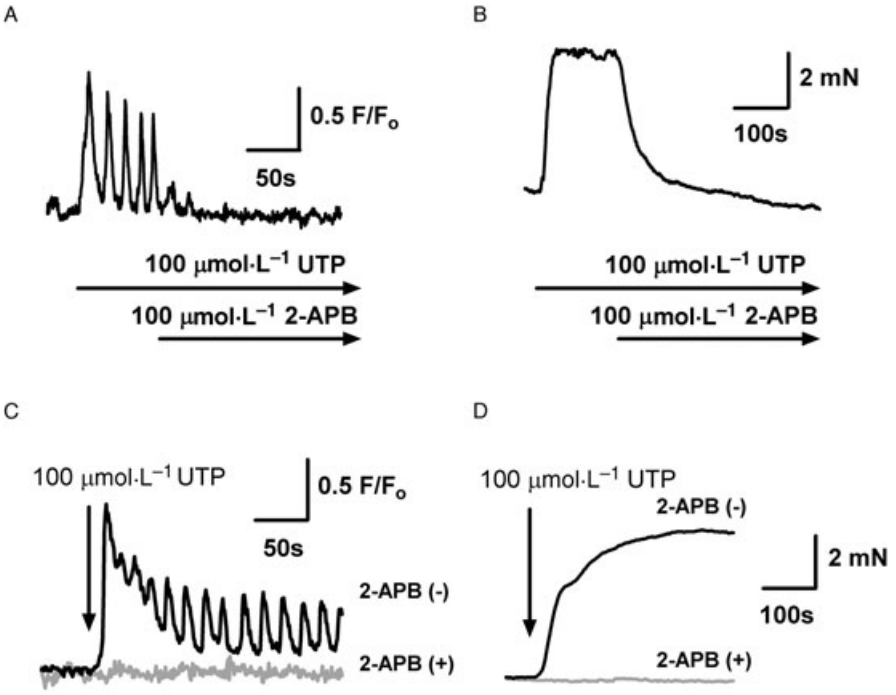

Figure 8 Effect of 2-aminoethoxydiphenylborate (2-APB) on uridine 5′-triphosphate (UTP)-induced Ca^{2+} waves and tonic contraction. (A) The application of 2-APB (100 μmol·L^{-1}) immediately abolished UTP (100 μmol·L^{-1})-induced Ca^{2+} waves ($n = 31$ cells from five animals) (B) 2-APB (100 μmol·L^{-1}) decreased UTP (100 μmol·L^{-1})-induced tonic contraction to 3.4 ± 0.7% of the control level ($P < 0.001$, $n = 6$ animals). (C) UTP (100 μmol·L^{-1}) stimulation after pretreatment of vessels with 2-APB (100 μmol·L^{-1}) for 30 min failed to elicit a Ca^{2+} response ($P < 0.0001$, $n = 24$ cells from three animals). In contrast, control vessels, without 2-APB (100 μmol·L^{-1}) preincubation, displayed Ca^{2+} waves after UTP stimulation. (D) UTP (100 μmol·L^{-1}) stimulation after pretreatment of vessels with 2-APB (100 μmol·L^{-1}) for 30 min failed to induce contraction ($P < 0.0001$, $n = 5$ animals) compared with control vessels without 2-APB preincubation.

$n = 38$ cells from six animals) (Figure 7A). In parallel, CPA (10 μmol·L^{-1}) also produced a 79 ± 2% inhibition of the UTP-induced tonic contraction (Figure 7B, $P < 0.001$, $n = 5$ animals).

Ca^{2+} release from the SR can be mediated through either the IP_3R and/or the RyR. 2-APB (100 μmol·L^{-1}), an inhibitor of IP_3Rs in VSMCs (Missiaen *et al.*, 2001), was used to examine the role of IP_3Rs in UTP-induced Ca^{2+} waves. Addition of 2-APB (100 μmol·L^{-1}) to ongoing Ca^{2+} waves immediately abolished them ($n = 31$ cells from five animals), and inhibited tonic contraction to 3.4 ± 0.7% of the control level ($P < 0.001$, $n = 6$ animals) (Figure 8A,B). Furthermore, UTP (100 μmol·L^{-1}) failed to elicit a Ca^{2+} transient or contraction in basilar arteries pre-incubated for 30 min with 2-APB (100 μmol·L^{-1}; Figure 8C,D).

It therefore appears that the opening of the IP_3Rs is required for UTP-mediated vasoconstriction and Ca^{2+} waves. However, as the specificity of 2-APB has been questioned, it was important to examine the selectivity of 2-APB in our preparation, especially with regard to Ca^{2+} translocators such as RyRs, sarco(endo)plasmic reticulum Ca^{2+} ATPase, the store-operated channels and the L-type Ca^{2+} channels. As shown in

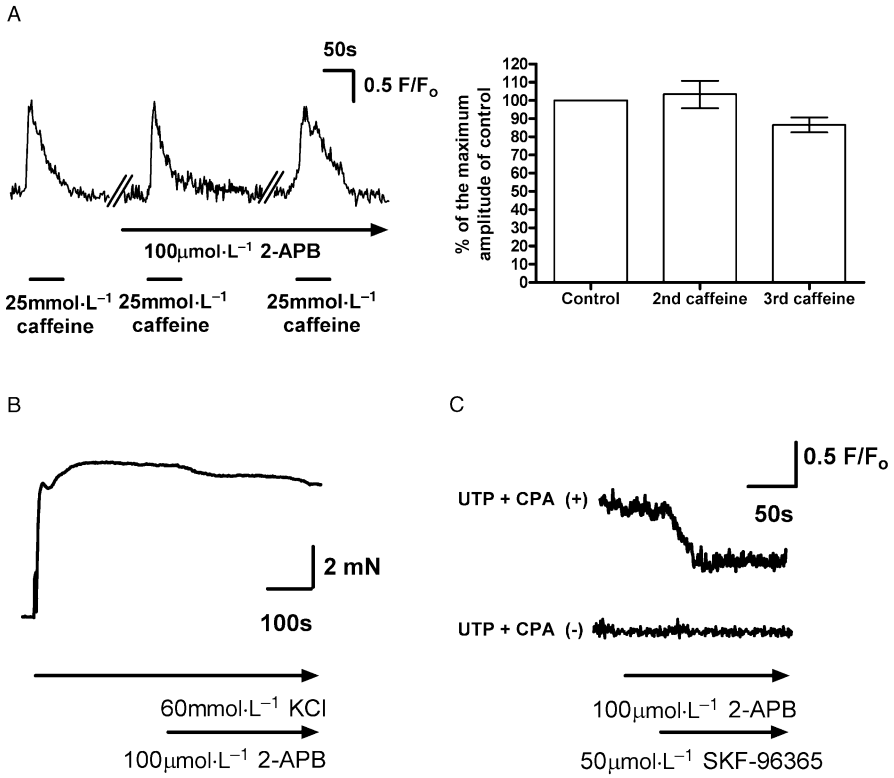

Figure 9 Effects of 2-aminoethoxydiphenylborate (2-APB) on the ryanodine-sensitive sarcoplasmic reticulum (SR) Ca^{2+} release channels, sarco(endo)plasmic reticulum Ca^{2+} ATPase, L-type Ca^{2+} channels and store-operated channels in rat basilar artery. (A) Left: Three pulses of caffeine (25 mmol·L^{-1}) were applied with a 5 min interval (breaks in record) between each pulse. Maximum amplitude of the caffeine-induced Ca^{2+} transient from the first pulse reflects control SR Ca^{2+} level as Ca^{2+} from the SR is released through the opened RyR channels. After the addition of 2-APB (100 μmol·L^{-1}), the second pulse of caffeine resulted in a single Ca^{2+} transient whose maximum amplitude is similar to the first pulse ($P = 0.66$, $n = 6$ animals). The third pulse of caffeine resulted in a Ca^{2+} transient whose maximum amplitude was slightly, but not significantly, diminished compared with the first pulse ($P = 0.11$, $n = 6$ animals). Right: Bar graph comparing the average maximum amplitude of the second and third caffeine pulses to the third pulse ($n = 6$ animals). (B) Application of 2-APB (100 μmol·L^{-1}) reduced tonic contraction induced by 60 mmol·L^{-1} KCl by 14.8 ± 4.3% ($P = 0.041$, $n = 6$ animals). (C) Application of uridine 5′-triphosphate (UTP) (100 μmol·L^{-1}) followed by cyclopiazonic acid (CPA) (10 μmol·L^{-1}) resulted in a maintained elevation in Ca^{2+} (upper panel). Application of 2-APB (100 μmol·L^{-1}) did not affect this plateau response, whereas the addition of SKF-96365 (50 μmol·L^{-1}) abolished the maintained Ca^{2+} elevation and returned to pre-stimulation baseline level (lower panel). Representative trace shown is typical of the responses obtained in 30 cells from four rats. RyR, ryanodine receptor.

Figure 9A, pretreatment with 2-APB (100 μmol·L^{-1}) did not significantly affect the peak amplitude of caffeine (25 mmol·L^{-1})-induced Ca^{2+} release (103 ± 8% of the control, $P = 0.66$, $n = 5$ animals), and therefore appears to be inactive against RyRs. Furthermore, 2-APB marginally affected SR refilling, as the peak amplitude of the third caffeine-induced Ca^{2+} transient was decreased slightly, but not significantly by 13.4 ± 4.1% ($P = 0.11$, $n = 6$ animals).

To test for direct effects on Ca^{2+} entry pathways, the effects of 2-APB on L-type Ca^{2+} channels and store-operated channels, two plasmalemmal channels important to UTP-mediated Ca^{2+} waves, were examined. 2-APB (100 μmol·L^{-1}) reduced 60 mmol·L^{-1} KCl-induced tonic contraction by 14.8 ± 4.3% (Figure 9B, $P = 0.041$, $n = 6$ animals). However, this slight inhibition of L-type Ca^{2+} channels cannot account for the complete inhibition of UTP-induced tonic contraction by 2-APB, as blockade of L-type Ca^{2+} channels with nifedipine only reduced force by 52%.

In addition to L-type Ca^{2+} channels, store-operated channels are also important for maintaining the Ca^{2+} waves. 2-APB has been reported to have non-selective effects on store-operated channels (Bootman *et al.*, 2002). The vessel was first stimulated with UTP (100 μmol·L^{-1}) to generate sustained Ca^{2+} waves, and then CPA (10 μmol·L^{-1}) was applied to inhibit SR Ca^{2+} reuptake, resulting in a maintained elevation of $[Ca^{2+}]_i$ and depletion of the SR (Figure 9C). The application of 2-APB (100 μmol·L^{-1}) did not affect the $[Ca^{2+}]_i$ plateau, although Ca^{2+} returned to baseline upon the subsequent addition of the store-operated channel blocker SKF-96365 (50 μmol·L^{-1}), indicating that in this preparation 2-APB does not inhibit the store-operated channels directly.

Although the opening of IP_3Rs are required for UTP-mediated Ca^{2+} waves and contraction, it does not rule out Ca^{2+} release through the RyR, another type of SR Ca^{2+} release channel which is functionally important in VSMCs. To assess the involvement of RyRs, high-concentration ryanodine (200 μmol·L^{-1}) and tetracaine (100 μmol·L^{-1}) were used to lock RyRs in their closed configuration. Neither ryanodine nor tetracaine had any effect on the frequency of the ongoing UTP-induced Ca^{2+} waves ($P = 0.67$, $n = 33$ cells from five animals; $P = 0.71$, $n = 29$ cells from four animals respectively) or tonic contraction ($P = 0.64$, $n = 5$ animals; $P = 0.64$, $n = 6$

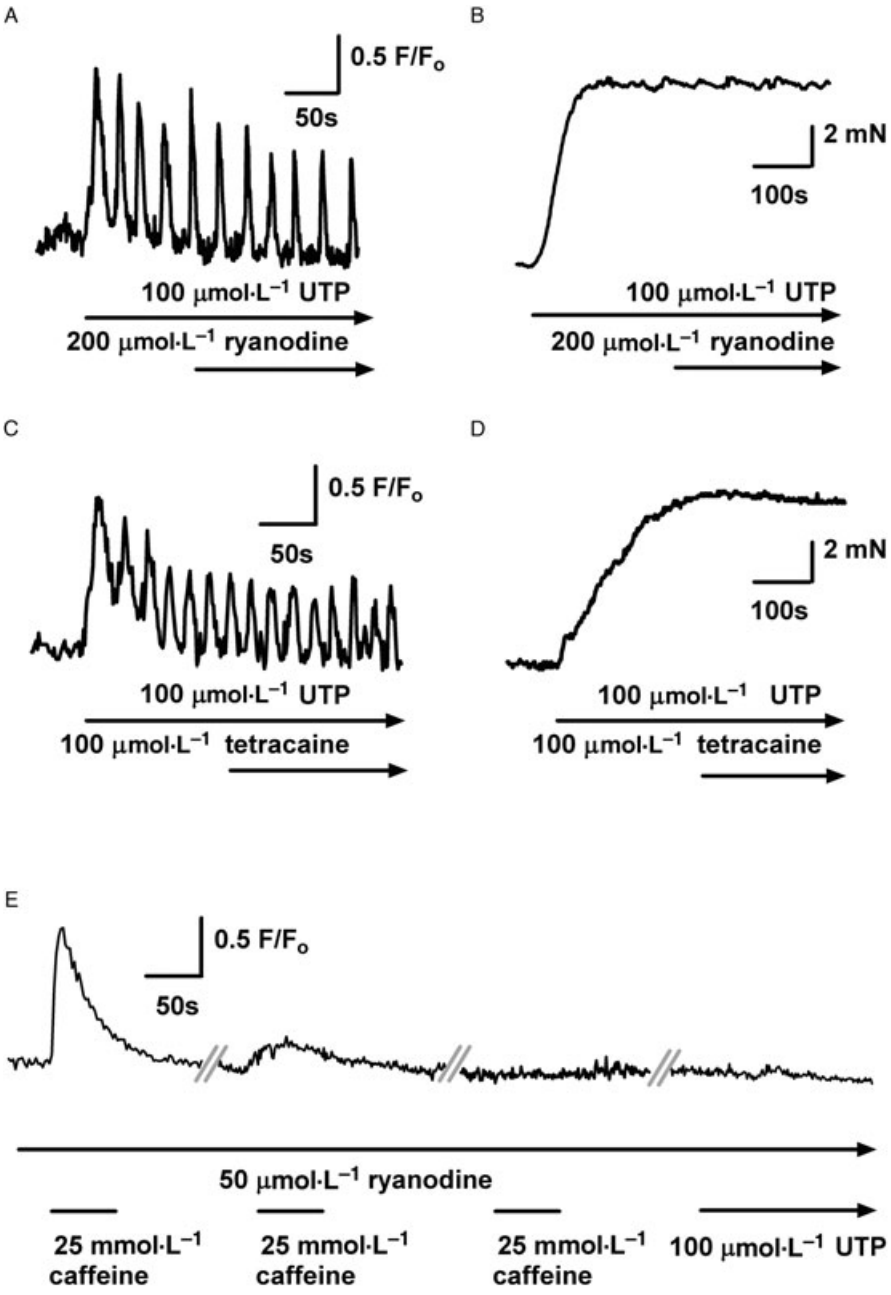

Figure 10 Effect of ryanodine, tetracaine and caffeine-induced depletion of sarcoplasmic reticulum (SR) Ca^{2+} stores on uridine 5′-triphosphate (UTP)-induced Ca^{2+} waves and tonic contraction in rat basilar artery. (A) Application of a high concentration (200 μmol·L^{-1}) of ryanodine did not affect ongoing UTP-induced Ca^{2+} waves ($P = 0.67$, $n = 33$ cells from five animals) (B) Ryanodine (200 μmol·L^{-1}) also did not affect UTP-induced tonic contraction ($P = 0.71$, $n = 5$ animals). (C) High concentrations (100 μmol·L^{-1}) of tetracaine also did not affect ongoing UTP-induced Ca^{2+} waves ($P = 0.71$, $n = 29$ cells from four animals) (D) Tetracaine (100 μmol·L^{-1}) had no significant effect on UTP-induced tonic contraction ($P = 0.64$, $n = 5$ animals). (E) To determine effects of depletion of RyR-sensitive SR Ca^{2+} stores, the artery was exposed to three 1 min treatments of caffeine (25 mmol·L^{-1}) in the continuous presence of ryanodine (50 μmol·L^{-1}) resulted in depletion of SR Ca^{2+} stores. The second stimulation of caffeine produced a much reduced Ca^{2+} transient, while the third stimulation produced no Ca^{2+} response. After depletion of SR Ca^{2+} stores, stimulation with UTP (100 μmol·L^{-1}) in the presence of ryanodine failed to elicit a Ca^{2+} response. Breaks in the record indicate a 5 min interval. RyR, ryanodine receptor.

animals) (Figure 10A,B,C,D). This supported the notion that Ca^{2+} release from the RyR-dependent SR store is not responsible for the generation of Ca^{2+} waves. To explore this issue further, RyRs were locked in the subconductance state by preincubation with ryanodine (50 μmol·L^{-1}) followed by a brief (1 min) exposure to caffeine (25 mmol·L^{-1}). The first caffeine exposure caused a transient Ca^{2+} response, whereas a second exposure elicited a much-reduced Ca^{2+} transient, and the third failed to elicit any Ca^{2+} transient at all (Figure 10E). We interpreted the final lack of Ca^{2+} transient in response to caffeine to indicate that release of Ca^{2+} through RyRs on the SR was no longer possible due to depletion of SR Ca^{2+} content and/or the locking of RyRs in an open state. UTP (100 μmol·L^{-1}) stimulation immediately after depletion of the

RyR-sensitive store no longer elicited a Ca^{2+} response. These results suggest that IP_3Rs and RyRs have access to a common SR Ca^{2+} store, but that opening of RyRs do not appear to be critical for the maintenance of UTP-induced Ca^{2+} waves.

Discussion

The concept that tonic vasoconstriction is based on asynchronous Ca^{2+} waves in individual smooth muscle cells has had a profound impact on our views on the molecular mechanisms underlying Ca^{2+} signalling in smooth muscle. The presence of agonist-induced Ca^{2+} waves in cerebral arteries has been documented by various groups (Jaggar and Nelson, 2000; Jaggar, 2001; Heppner *et al.*, 2002), but a detailed investigation of their underlying mechanisms has not yet been conducted. We have investigated the link between agonist-induced Ca^{2+} waves and tonic contraction using an *in situ* preparation of the rat basilar artery and have systematically studied the ionic mechanisms underlying these Ca^{2+} waves, which appear to be similar to those described in VSM from larger conduit blood vessels (Lee *et al.*, 2002). Our studies of UTP-induced Ca^{2+} waves were performed in isometrically stretched arteries, which are similar to the conditions in which UTP-induced Ca^{2+} waves were first described (Jaggar and Nelson, 2000), and may shed new light on how wall tension may be regulated in the basilar artery.

The response to UTP is typified by repetitive transient elevations in Ca^{2+} which originate in distinct intracellular foci and then spread out as waves over the length of the smooth muscle cell. The cells respond independently of each other in that the Ca^{2+} waves are asynchronous, and the cells vary in their sensitivity to UTP, such that recruitment of responding cells increases with increasing UTP concentration. Furthermore, the propagation velocity and frequency also increases with increasing UTP concentration (Figure 1C,D). Functionally, it appears that Ca^{2+} waves underlie tonic contraction, as their inhibition with nifedipine, SKF-96365, KB-R7943, or 2-APB is associated with complete inhibition of force (Figures 4, 5 and 8). Finally, the lack of synchronicity between neighbouring VSMCs explains how summation of individual-cell Ca^{2+} waves can lead to tonic contraction, as the summation of Ca^{2+} signals in all the cells averages out to be a steady-state Ca^{2+} increase in whole vessels (Ruehlmann *et al.*, 2000; Mauban *et al.*, 2001). The apparent importance of Ca^{2+} waves for tonic contraction is further demonstrated when their abolition by CPA markedly reduces force by 80%, although the average $[Ca^{2+}]_i$ remains significantly elevated above baseline (Figure 7). This indicates a higher force-to-$[Ca^{2+}]_i$ ratio when VSMCs are activated with Ca^{2+} waves as compared with sustained $[Ca^{2+}]_i$, suggesting that Ca^{2+} waves represent a more efficient method to deliver Ca^{2+} to activate myosin light-chain kinase, which is tethered to the contractile filaments (Lee *et al.*, 2001; Wilson *et al.*, 2002). However, ultimately contraction is determined by the level of phosphorylation of myosin light chain (MLC) which is both Ca^{2+}-dependent and Ca^{2+}-independent (Weber *et al.*, 1999). The way in which Ca^{2+} waves, as opposed to a steady state elevation of Ca^{2+}, might be related to this level of phosphorylation is as yet unknown. Further studies are needed to determine the underlying physiological explanation of how Ca^{2+} waves signal for contraction.

The UTP-induced Ca^{2+} waves appear to be propagated by regenerative Ca^{2+} release from the SR network, as depletion of SR Ca^{2+} stores with CPA abolishes the Ca^{2+} waves (Figure 7). Extracellular Ca^{2+} influx appears to be critical for the maintenance of Ca^{2+} waves, although the ability of Ca^{2+} waves to persist for a time in the absence of Ca^{2+} is likely to be due to several Ca^{2+} transport mechanisms. In smooth muscle, a proportion of the Ca^{2+} released by the SR is inevitably extruded to the extracellular space by the actions of the plasma membrane Ca^{2+} ATPase, and in a Ca^{2+}-free medium all Ca^{2+} release from the SR is irreversibly lost to the extracellular space (Leijten and van Breemen, 1986). However, removal of Ca^{2+} towards the extracellular space is in competition with SR Ca^{2+} reuptake through the sarco(endo)plasmic reticulum Ca^{2+} ATPase, which allows the SR to continue releasing decreasing amounts of Ca^{2+} to sustain the Ca^{2+} waves. Finally, a third mechanism of Ca^{2+} unloading of the SR during Ca^{2+}-free conditions is the transfer of Ca^{2+} release by the peripheral RyRs towards the forward-mode (Ca^{2+}-extrusion) Na^+/Ca^{2+} exchange, a mechanism which as been described in both VSMCs and endothelial cells (Nazer and van Breemen, 1998; Liang *et al.*, 2004). Therefore, without refilling of the SR, all of the Ca^{2+} is eventually extruded resulting in the disappearance of the Ca^{2+} waves.

Influx of extracellular Ca^{2+} through L-type Ca^{2+} channels is central in the control of cerebrovascular arterial diameter (Nelson *et al.*, 1990). However, it is interesting that the UTP-induced Ca^{2+} waves were not abolished by nifedipine, but only reduced in frequency. One mechanism through which frequency could be decreased is that the absence of stimulated Ca^{2+} influx through L-type Ca^{2+} channels may reduce the rate of refilling of the SR Ca^{2+} store. As SR luminal Ca^{2+} can regulate IP_3R channel opening probability, a reduced rate of SR Ca^{2+} refilling can result in a decreased frequency of SR Ca^{2+} release at the wave initiation site (Meldolesi and Pozzan, 1998). Similarly, blockade of L-type Ca^{2+} channels in pressurized mouse mesenteric arteries, which abolished myogenic tone, also reduced the frequency of phenylephrine-induced Ca^{2+} waves (Zacharia *et al.*, 2007). However, pressure-induced Ca^{2+} waves in small rat cerebral arteries were completely abolished with diltiazem (Jaggar, 2001). Although the larger cerebral vessels, such as the basilar artery, share some properties of resistance vessels (Toyoda *et al.*, 1996), these differing observations may be the result of tissue differences, with respect to relative involvement of the various Ca^{2+} entry mechanisms. Furthermore, these apparent mechanistic differences may also be attributed to different physiological conditions, for example pressurization versus tension. For example, the development of myogenic tone may influence the Ca^{2+} signal elicited by agonists (Zacharia *et al.*, 2007). Consequently, comparisons between the mechanisms of Ca^{2+} waves must take differences in vascular beds and experimental preparations into consideration.

Another major finding in this study is that UTP-induced Ca^{2+} waves are abolished by KB-R7943, an inhibitor of reverse-mode Na^+/Ca^{2+} exchanger-mediated Ca^{2+} entry across the plasma membrane (Iwamoto *et al.*, 1996; Ladilov *et al.*, 1999). The plasma membrane Na^+/Ca^{2+} exchanger is a transmembrane protein that normally couples the influx of Na^+ ions to the efflux of Ca^{2+} ions in a 3:1 ratio (Philipson and Nicoll, 2000). However, Na^+ entry through receptor- and store-

operated channels which are functionally coupled to the Na^+/Ca^{2+} exchanger may influence the dynamics of Na^+/Ca^{2+} exchange, as Na^+ accumulates regionally in a restricted sub-plasmalemmal space between the superficial SR and the plasma membrane (Arnon *et al.*, 2000; Poburko *et al.*, 2004; Lemos *et al.*, 2007). This build-up in subcellular Na^+ was hypothesized to change the electrochemical gradient to favour Ca^{2+} influx through reversal of the Na^+/Ca^{2+} exchanger, which in turn refills the SR Ca^{2+} stores (Lee *et al.*, 2001). This would explain our findings that the nifedipine-resistant Ca^{2+} waves and tonic contraction are similarly sensitive to both SKF-96365, an inhibitor of store- and receptor-operated channels, and KB-R7943.

However, to achieve reversal of the Na^+/Ca^{2+} exchanger, the subplasmalemmal Na^+ concentration ($[Na^+]_{subPM}$) must reach at least the level of the K_m of the exchanger. Although the $[Na^+]_{subPM}$ has not been measured in this preparation, we have predicted from our studies with rat aortic smooth muscle cells that reverse-mode Na^+/Ca^{2+} exchange should occur when $[Na^+]_{subPM}$ exceeds 23–25 mmol·L^{-1}, assuming $E_m = -60$ mV, $E_{NCX} = 3E_{Na} - 2E_{Ca}$, $[Ca^{2+}]_o = 1.2$ mmol·L^{-1}, $[Ca^{2+}]_{subPM} = 500$ μmol·L^{-1} and $[Na^+]_o = 145$ mmol·L^{-1} (where $[Ca^{2+}]_o$ = extracellular $[Ca^{2+}]$, $[Ca^{2+}]_{subPM}$ = sub-plasmalemmal $[Ca^{2+}]$, and $[Na^+]_o$ = extracellular $[Na^+]$) (Poburko *et al.*, 2006). Recently, Poburko *et al.* provided the first direct demonstration of localized subcellular increases in Na^+ through receptor-operated/store-operated channels to ≥30 mmol·L^{-1} (Poburko *et al.*, 2007), which is consistent with estimates of Na^+ ranging from 24 to 40 mmol·L^{-1} in ventricular myocytes (Wendt-Gallitelli *et al.*, 1993; Isenberg *et al.*, 2003). In addition, the space constant for the sub-plasmalemmal Na^+ gradient in ventricular myocytes is 28 nm, which is highly consistent with the intermembrane separation (~20 nm) in PM-SR junctions in the rat basilar artery preparation (unpublished observations). Furthermore, given that the resting membrane potential in rat basilar artery is approximately −43 mV (Haddock and Hill, 2002), and that a more depolarized membrane decreases $[Na^+]_{subPM}$ required for reversal of Na^+/Ca^{2+} exchange, it seems plausible that reverse-mode Na^+/Ca^{2+} exchange is a physiological route of Ca^{2+} entry in cerebral arteries. This is especially relevant as our finding that KB-R7943 abolishes Ca^{2+} waves suggests that SR refilling is critically dependent on reverse-mode Na^+/Ca^{2+} exchange during UTP stimulation (Figure 5C). Although it remains to be investigated, this may serve as an example of privileged delivery of Ca^{2+} from a transport site located in one membrane to a second Ca^{2+} transport site in an apposing membrane, a process which serves to circumvent free diffusion throughout the cytoplasm (Poburko *et al.*, 2004; Fameli *et al.*, 2007). In addition to its inhibition of reverse-mode Na^+/Ca^{2+} exchange, KB-R7943 has been also been reported to have effects on L-type Ca^{2+} and store-operated channels, neuronal nicotinic acetylcholine receptors, the N-methyl-D-aspartic acid (NMDA) receptor and the noradrenaline transporter (Watano *et al.*, 1996; Sobolevsky and Khodorov, 1999; Arakawa *et al.*, 2000; Iwamoto, 2004). However, in our preparation, KB-R7943 does not significantly inhibit L-type Ca^{2+} channels or store-operated channels, which supported the notion that it is the reverse-mode Na^+/Ca^{2+} exchange, which is important in refilling the SR to maintain Ca^{2+} waves.

Uridine 5'-triphosphate exerts its effects on metabotropic purinergic P2Y receptors, and has been shown to augment Ca^{2+} release via an increase in cytoplasmic inositol 1,4,5-trisphosphate [Ins(1,4,5)P_3] (Strobaek *et al.*, 1996; Sima *et al.*, 1997). To investigate the role of IP_3Rs, we used 2-APB, a small molecular weight membrane permeable modulator of the IP_3R (Missiaen *et al.*, 2001). However, its use to block IP_3Rs has been criticized for its non-specific effects on other ion transport mechanisms, notably its inhibition of store-operated channels (Broad *et al.*, 2001; Ma *et al.*, 2001; Ratz and Berg, 2006). Importantly in our preparation, 2-APB immediately abolished ongoing Ca^{2+} waves and tonic contraction, and did not affect caffeine-releasable Ca^{2+} stores, which is consistent with an action of 2-APB to block IP_3Rs (Figure 9A). Furthermore, pre-incubation with 2-APB did not elicit a Ca^{2+} response or contraction. It also had only a minor non-significant effect on SR Ca^{2+} reuptake. 2-APB caused no significant inhibition of store-operated channels and, although it does affect L-type Ca^{2+} channels, the slight inhibition observed could not have accounted for the abolition of Ca^{2+} waves (Figure 9B,C). Therefore, our findings support the notion that opening of IP_3R channels is not only responsible for the initial Ca^{2+} release, but is also required for subsequent regenerative release of Ca^{2+} underlying the propagation of the Ca^{2+} waves. Acetylcholine-induced Ca^{2+} waves in rat portal vein myocytes are also dependent on activation of IP_3Rs, although interestingly the IP_3R2 subtype, which is most sensitive to Ca^{2+}, appears to be most important for the propagation of Ca^{2+} waves (Morel *et al.*, 2003; Fritz *et al.*, 2008). It should also be noted that the Ca^{2+} waves are maintained by the intrinsic sensitivity of the IP_3R2 subtype to cytosolic $[Ca^{2+}]_i$, and not due to oscillation of Ins(1,4,5)P_3 levels (Fritz *et al.*, 2008). A possible scenario in the rat basilar artery is that UTP-induced Ca^{2+} wave begins with elevation of Ins(1,4,5)P_3. The Ins(1,4,5)P_3 sensitizes the IP_3R to Ca^{2+}, and when Ca^{2+} reaches a threshold concentration, the release channels open (Streb *et al.*, 1983; Ferris *et al.*, 1992). As the concentration of UTP is raised, the concentrations of Ins(1,4,5)P_3 and basal $[Ca^{2+}]_i$ are also raised, which shortens the time required for Ca^{2+} to reach threshold value for the initiation of the next wave. The regenerative nature depends on the positive feedback of increasing Ca^{2+} on the Ins(1,4,5)P_3 sensitivity of IP_3R. This mechanism, combined with the fact that $InsP_3$ sensitizes the IP_3R to Ca^{2+}, ensures that both the frequency and velocity increase with increasing UTP concentration. However, knowledge of the Ins(1,4,5)P_3 dynamics in our preparation is required before this mechanism can be established.

The observed effect of 2-APB indicates an essential role of IP_3Rs in the initiation and maintenance of UTP-induced Ca^{2+} waves, but does not exclude involvement of RyRs. Although there is general agreement that the initiation of oscillations and waves is a response to agonists acting on sarcolemmal receptors which releases Ca^{2+} from the SR via IP_3Rs, controversy remains whether or not Ca^{2+} release from the IP_3Rs then activates RyRs to generate further release by Ca^{2+}-induced Ca^{2+}-release and to propagate waves, or whether the entire release process arises from IP_3Rs without significant RyR involvement (Mccarron *et al.*, 2003). The former proposal is supported by studies which showed that drugs which block RyRs often abolish Ca^{2+} oscillations initiated by Ins(1,4,5)P_3-generating agonists (Hyvelin *et al.*, 1998; Boittin

et al., 1999; Jaggar and Nelson, 2000). This is possibly due to co-localization of RyRs and IP_3Rs, which allows Ca^{2+} released locally by IP_3Rs to activate adjacent clusters of RyRs by Ca^{2+}-induced Ca^{2+} release (Gordienko and Bolton, 2002). On the other hand, some preparations which lack a Ca^{2+}-induced Ca^{2+} release mechanism still exhibit Ca^{2+} waves (DeLisle and Welsh, 1992; Lechleiter and Clapham, 1992). Furthermore, in pressurized rat mesenteric artery, RyRs do not appear to play a role in agonist-stimulated Ca^{2+} waves (Lamont and Wier, 2004). It is important to note here that many studies which utilize pharmacological tools to inhibit RyRs, such as the plant alkaloid ryanodine, are complicated by the concentration-dependent effects in different tissues. For example, low concentrations (<100 $\mu mol \cdot L^{-1}$) of ryanodine cause persistent opening of the channels which may lead to store depletion (Rousseau *et al.*, 1987, Kanmura *et al.*, 1988, Xu *et al.*, 1994), while higher concentrations are reported to lock RyRs in a closed state to inhibit Ca^{2+} release (Fill and Copello, 2002). Furthermore, the drugs may also block Ins(1,4,5)P_3-mediated Ca signals themselves (either directly or indirectly) without RyR involvement in Ca^{2+} increase.

In our preparation, depletion of the RyR-sensitive Ca^{2+} stores using a combination of caffeine and low concentration of ryanodine to lock the RyRs in a subconductance state eliminated the ability of UTP to induce Ca^{2+} waves (Figure 10). The concentration of ryanodine (50 $\mu mol \cdot L^{-1}$) we used which is greater than the concentration which is known to lock RyRs in an open state in smooth muscle (Iino *et al.*, 1988; Kanmura *et al.*, 1988). This suggests that the IP_3R and RyR both access a common SR Ca^{2+} store such that the depletion of RyR stores prevents Ca^{2+} waves, as has been demonstrated (Lepretre and Mironneau, 1994; McCarron and Olson, 2008), but does not prove that RyRs participate in the propagation of Ca^{2+} waves. Therefore, we used a high concentration of ryanodine (200 $\mu mol \cdot L^{-1}$) to lock the RyRs in the closed-configuration and found that UTP-induced Ca^{2+} waves were not affected (Figure 10). Additionally, we used tetracaine (200 $\mu mol \cdot L^{-1}$), which is not dependent on the opening of RyRs to exert their effects, and also found that the Ca^{2+} waves were not affected (Györke *et al.*, 1997). This is in contrast to the rat cerebral arteries, where ryanodine (10 $\mu mol \cdot L^{-1}$) inhibited UTP-induced Ca^{2+} waves (Jaggar and Nelson, 2000). However, it should be noted that in the same preparation, ryanodine also inhibited Ca^{2+} sparks, most likely as a result of SR Ca^{2+} store depletion. Additionally, another possibility is that in our preparation and in others, the RyRs do not play a role because they are not localized near the IP_3Rs. However, well-controlled double-labeling of the IP_3Rs and RyRs at electron microscopic resolutions is required before such a conclusion can be made.

It is interesting to note that the mechanism of UTP-induced asynchronous Ca^{2+} waves elicited in this study shares some similarities to the mechanism of Ca^{2+} oscillations underlying spontaneous vasomotion, as they were not abolished by nifedipine, dependent on a functional SR, and were abolished by antagonists of IP_3 (Haddock and Hill, 2002; 2005). This is more significant in light of the fact that asynchronous Ca^{2+} waves often precede the rhythmic contraction of blood vessels, or vasomotion, which has been observed to occur spontaneously or in response to high concentrations of agonist stimulation, and may have physiological and pathophysiological importance (Gratton *et al.*, 1998; Hudetz *et al.*, 1998, Shimamura *et al.*, 1999; Rücker *et al.*, 2000). In agonist-stimulated vasomotion, asynchronous Ca^{2+} waves are first initiated without the generation of tension. In the presence of the endothelium, the periodic increases in $[Ca^{2+}]_i$ activate cGMP-dependent, Ca^{2+}-sensitive Cl^- channels, which cause Cl^- currents which depolarize the membrane periodically. The depolarization spreads rapidly through neighbouring cells and activates L-type Ca^{2+} channels, facilitating Ca^{2+} influx which facilitates Ca^{2+}-induced Ca^{2+}-release to initiate the next Ca^{2+} wave, which will then occur simultaneously in all the nearby smooth muscle cells and generate oscillatory vasomotion (Peng *et al.*, 2001; Rahman *et al.*, 2005).

Similarly, with spontaneous vasomotion, the trigger for synchronicity of Ca^{2+} waves is thought to be due to the activation of a chloride-dependent Ca^{2+} channel (Haddock and Hill, 2002). The resulting depolarization then spreads quickly to neighbouring cells, such that L-type Ca^{2+} channels are simultaneously activated. The resulting Ca^{2+} influx then facilitates Ca^{2+}-induced Ca^{2+} release to initiate a synchronous Ca^{2+} release and contraction. In the study by Haddock and Hill (2002), synchronized Ca^{2+} waves were abolished upon blockade of L-type Ca^{2+} channels with nifedipine, but asynchronous Ca^{2+} oscillations persisted in individual cells, which supports the hypothesis that the entrainment of L-type Ca^{2+} channels are important in synchronized Ca^{2+} oscillations. Synchronization of Ca^{2+} oscillations between VSMCs underlying vasomotion is critically dependent on the coordination of Ca^{2+} signals within individual VSMCs leading to synchronized Ca^{2+} responses and the development of simultaneous contractions along the vessel length (Christ *et al.*, 1996). In small vessels, this coordination may be dependent on an intact endothelium, which may be one reason why we did not observe synchronized Ca^{2+} waves upon UTP stimulation in our preparation (Haddock and Hill, 2005).

In summary, the data presented in this article show that several different Ca^{2+} translocating proteins are involved in the generation of Ca^{2+} waves in UTP-stimulated smooth muscle cells of the rat basilar artery. These Ca^{2+} waves appear to be produced by repetitive cycles of SR Ca^{2+} release which are mediated by IP_3Rs, followed by sarco(endo)plasmic reticulum Ca^{2+}-ATPase-mediated SR Ca^{2+} reuptake of Ca^{2+} entry involving L-type Ca^{2+} channels, receptor/store-operated channels and reverse-mode Na^+/Ca^{2+} exchange. In general, the mechanisms of the Ca^{2+} waves in the basilar artery are similar to those in the large conduit vessels, which may indicate a common Ca^{2+} signalling mechanism which initiates and sustains Ca^{2+} waves in the vasculature.

Acknowledgements

This work was partly funded by the Canadian Institutes of Health Research. HS is a recipient of the Michael Smith Foundation for Health Research and National Sciences and Engineering Research Council Trainee Awards.

Conflict of interest

None.

References

Alexander SPH, Mathie A, Peters JA (2008). Guide to Receptors and Channels (GRAC), 3rd edition (2008 revision). *Br J Pharmacol* **153** (Suppl. 2): S1–S209.

Arakawa N, Sakaue M, Yokoyama I, Hashimoto H, Koyama Y, Baba A *et al*. (2000). KB-R7943 inhibits store-operated Ca(2+) entry in cultured neurons and astrocytes. *Biochem Biophys Res Commun* **279**: 354–357.

Arnon A, Hamlyn JM, Blaustein MP (2000). Na(+) entry via store-operated channels modulates Ca(2+) signaling in arterial myocytes. *Am J Physiol Cell Physiol* **278**: C163–C173.

Asada Y, Yamazawa T, Hirose K, Takasaka T, Iino M (1999). Dynamic Ca2+ signalling in rat arterial smooth muscle cells under the control of local renin-angiotensin system. *J Physiol* **521**: 497–505.

Boarder MR, Hourani SM (1998). The regulation of vascular function by P2 receptors: multiple sites and multiple receptors. *Trends Pharmacol Sci* **19**: 99–107.

Boittin FX, Macrez N, Halet G, Mironneau J (1999). Norepinephrine-induced Ca(2+) waves depend on InsP(3) and ryanodine receptor activation in vascular myocytes. *Am J Physiol* **277**: C139–C151.

Bolton TB (1979). Mechanisms of action of transmitters and other substances on smooth muscle. *Physiol Rev* **59**: 606–718.

Bootman MD, Collins TJ, Mackenzie L, Roderick HL, Berridge MJ, Peppiatt CM (2002). 2-aminoethoxydiphenyl borate (2-APB) is a reliable blocker of store-operated Ca2+ entry but an inconsistent inhibitor of InsP3-induced Ca2+ release. *FASEB J* **16**: 1145–1150.

Broad LM, Braun FJ, Lievremont JP, Bird GS, Kurosaki T, Putney JW Jr (2001). Role of the phospholipase C-inositol 1,4,5-trisphosphate pathway in calcium release-activated calcium current and capacitative calcium entry. *J Biol Chem* **276**: 15945–15952.

Burnstock G (1998). History of extracellular nucleotides and their receptors. In: Turner JT, Weisman GA, Fedan JS (eds). *The P2 Nucleotide Receptors*. Humana Press: Totowa, NJ, pp. 3–40.

Christ GJ, Spray DC, el-Sabban M, Moore LK, Brink PR (1996). Gap junctions in vascular tissues. Evaluating the role of intercellular communication in the modulation of vasomotor tone. *Circ Res* **79**: 631–646.

Debdi M, Seylaz J, Sercombe R (1992). Early changes in rabbit cerebral artery reactivity after subarachnoid hemorrhage. *Stroke* **23**: 1154–1162.

DeLisle S, Welsh MJ (1992). Inositol trisphosphate is required for the propagation of calcium waves in Xenopus oocytes. *J Biol Chem* **267**: 7963–7966.

Fameli N, van Breemen C, Kuo KH (2007). A quantitative model for linking Na+/Ca2+ exchanger to SERCA during refilling of the sarcoplasmic reticulum to sustain [Ca2+] oscillations in vascular smooth muscle. *Cell Calcium* **42**: 565–575.

Ferris CD, Cameron AM, Huganir RL, Snyder SH (1992). Quantal calcium release by purified reconstituted inositol 1,4,5-trisphosphate receptors. *Nature* **356**: 350–352.

Fill M, Copello JA (2002). Ryanodine receptor calcium release channels. *Physiol Rev* **82**: 893–922.

Fritz N, Mironneau J, Macrez N, Morel JL (2008). Acetylcholine-induced Ca(2+) oscillations are modulated by a Ca(2+) regulation of InsP (3)R2 in rat portal vein myocytes. *Pflugers Arch* **456**: 277–283.

Gordienko DV, Bolton TB (2002). Crosstalk between ryanodine receptors and IP(3) receptors as a factor shaping spontaneous Ca(2+)-release events in rabbit portal vein myocytes. *J Physiol* **542**: 743–762.

Gratton RJ, Gandley RE, McCarthy JF, Michaluk WK, Slinker BK, McLaughlin MK (1998). Contribution of vasomotion to vascular resistance: a comparison of arteries from virgin and pregnant rats. *J Appl Physiol* **85**: 2255–2260.

Györke S, Lukyanenko V, Györke I (1997). Dual effects of tetracaine on spontaneous calcium release in rat ventricular myocytes. *J Physiol* **500**: 297–309.

Haddock RE, Hill CE (2002). Differential activation of ion channels by inositol 1,4,5-trisphosphate (IP3)- and ryanodine-sensitive calcium stores in rat basilar artery vasomotion. *J Physiol* **545**: 615–627.

Haddock RE, Hill CE (2005). Rhythmicity in arterial smooth muscle. *J Physiol* **566**: 645–656.

Hardebo JE, Kahrstrom J, Owman C (1987). P1- and P2-purine receptors in brain circulation. *Eur J Pharmacol* **144**: 343–352.

Heppner TJ, Bonev AD, Santana LF, Nelson MT (2002). Alkaline pH shifts Ca2+ sparks to Ca2+ waves in smooth muscle cells of pressurized cerebral arteries. *Am J Physiol Heart Circ Physiol* **283**: H2169–H2176.

Horiuchi T, Dietrich HH, Tsugane S, Dacey RG Jr (2001). Analysis of purine- and pyrimidine-induced vascular responses in the isolated rat cerebral arteriole. *Am J Physiol Heart Circ Physiol* **280**: H767–H776.

Hudetz AG, Biswal BB, Shen H, Lauer KK, Kampine JP (1998). Spontaneous fluctuations in cerebral oxygen supply an introduction. *Adv Exp Med Biol* **454**: 551–559.

Hyvelin JM, Guibert C, Marthan R, Savineau JP (1998). Cellular mechanisms and role of endothelin-1-induced calcium oscillations in pulmonary arterial myocytes. *Am J Physiol* **275**: L269–L282.

Iino M, Kobayashi T, Endo M (1988). Use of ryanodine for functional removal of the calcium store in smooth muscle cells of the guinea-pig. *Biochem Biophys Res Commun* **152**: 417–422.

Iino M, Kasai H, Yamazawa T (1994). Visualization of neural control of intracellular Ca2+ concentration in single vascular smooth muscle cells in situ. *EMBO J* **13**: 5026–5031.

Isenberg G, Kazanski V, Kondratev D, Gallitelli MF, Kiseleva I, Kamkin A (2003). Differential effects of stretch and compression on membrane currents and [Na+]c in ventricular myocytes. *Prog Biophys Mol Biol* **82**: 43–56.

Iwamoto T (2004). Forefront of Na+/Ca2+ exchanger studies: molecular pharmacology of Na+/Ca2+ exchange inhibitors. *J Pharmacol Sci* **96**: 27–32.

Iwamoto T, Watano T, Shigekawa M (1996). A novel isothiourea derivative selectively inhibits the reverse mode of Na+/Ca2+ exchange in cells expressing NCX1. *J Biol Chem* **271**: 22391–22397.

Jaggar JH (2001). Intravascular pressure regulates local and global Ca(2+) signaling in cerebral artery smooth muscle cells. *Am J Physiol Cell Physiol* **281**: C439–C448.

Jaggar JH, Nelson MT (2000). Differential regulation of Ca(2+) sparks and Ca(2+) waves by UTP in rat cerebral artery smooth muscle cells. *Am J Physiol Cell Physiol* **279**: C1528–C1539.

Kanmura Y, Missiaen L, Raeymaekers L, Casteels R (1988). Ryanodine reduces the amount of calcium in intracellular stores of smooth-muscle cells of the rabbit ear artery. *Pflugers Arch* **413**: 153–159.

Ladilov Y, Haffner S, Balser-Schäfer C, Maxeiner H, Piper HM (1999). Cardioprotective effects of KB-R7943: a novel inhibitor of the reverse mode of Na+/Ca2+ exchanger. *Am J Physiol* **276**: H1868–H1876.

Lamont C, Wier WG (2004). Different roles of ryanodine receptors and inositol (1,4,5)-trisphosphate receptors in adrenergically stimulated contractions of small arteries. *Am J Physiol Heart Circ Physiol* **287**: H617–H625.

Lechleiter JD, Clapham DE (1992). Molecular mechanisms of intracellular calcium excitability in X. laevis oocytes. *Cell* **69**: 283–294.

Lee CH, Poburko D, Sahota P, Sandhu J, Ruehlmann DO, van Breemen C (2001). The mechanism of phenylephrine-mediated [Ca(2+)](i) oscillations underlying tonic contraction in the rabbit inferior vena cava. *J Physiol* **534**: 641–650.

Lee CH, Poburko D, Kuo KH, Seow CY, van Breemen C (2002). Ca(2+)

oscillations, gradients, and homeostasis in vascular smooth muscle. *Am J Physiol Heart Circ Physiol* **282**: H1571–H1583.

Leijten PA, van Breemen C (1986). The relationship between noradrenaline-induced contraction and 45Ca efflux stimulation in rabbit mesenteric artery. *Br J Pharmacol* **89**: 739–747.

Lemos VS, Poburko D, Liao CH, Cole WC, van Breemen C (2007). Na+ entry via TRPC6 causes Ca2+ entry via NCX reversal in ATP stimulated smooth muscle cells. *Biochem Biophys Res Commun* **352**: 130–134.

Lepretre N, Mironneau J (1994). Alpha 2-adrenoceptors activate dihydropyridine-sensitive calcium channels via Gi-proteins and protein kinase C in rat portal vein myocytes. *Pflugers Arch* **429**: 253–261.

Liang W, Buluc M, van Breemen C, Wang X (2004). Vectorial Ca2+ release via ryanodine receptors contributes to Ca2+ extrusion from freshly isolated rabbit aortic endothelial cells. *Cell Calcium* **36**: 431–443.

Ma HT, Venkatachalam K, Li HS, Montell C, Kurosaki T, Patterson RL *et al*. (2001). Assessment of the role of the inositol 1,4,5-trisphosphate receptor in the activation of transient receptor potential channels and store-operated Ca2+ entry channels. *J Biol Chem* **276**: 18888–18896.

McCarron JG, Olson ML (2008). A single luminally continuous sarcoplasmic reticulum with apparently separate Ca2+ stores in smooth muscle. *J Biol Chem* **283**: 7206–7218.

McCarron JG, Bradley KN, MacMillan D, Muir TC (2003). Sarcolemma agonist-induced interactions between InsP3 and ryanodine receptors in Ca2+ oscillations and waves in smooth muscle. *Biochem Soc Trans* **31**: 920–924.

Mauban JR, Lamont C, Balke CW, Wier WG (2001). Adrenergic stimulation of rat resistance arteries affects Ca(2+) sparks, Ca(2+) waves, and Ca(2+) oscillations. *Am J Physiol Heart Circ Physiol* **280**: H2399–H2405.

Meldolesi J, Pozzan T (1998). The endoplasmic reticulum Ca2+ store: a view from the lumen. *Trends Biochem Sci* **23**: 10–14.

Miriel VA, Mauban JR, Blaustein MP, Wier WG (1999). Local and cellular Ca2+ transients in smooth muscle of pressurized rat resistance arteries during myogenic and agonist stimulation. *J Physiol* **518**: 815–824.

Missiaen L, Callewaert G, De Smedt H, Parys JB (2001). 2-Aminoethoxydiphenyl borate affects the inositol 1,4,5-trisphosphate receptor, the intracellular Ca2+ pump and the non-specific Ca2+ leak from the non-mitochondrial Ca2+ stores in permeabilized A7r5 cells. *Cell Calcium* **29**: 111–116.

Morel JL, Fritz N, Lavie JL, Mironneau J (2003). Crucial role of type 2 inositol 1,4,5-trisphosphate receptors for acetylcholine-induced Ca2+ oscillations in vascular myocytes. *Arterioscler Thromb Vasc Biol* **23**: 1567–1575.

Nazer MA, van Breemen C (1998). Functional linkage of Na(+)-Ca2+ exchange and sarcoplasmic reticulum Ca2+ release mediates Ca2+ cycling in vascular smooth muscle. *Cell Calcium* **24**: 275–283.

Nelson MT, Patlak JB, Worley JF, Standen NB (1990). Calcium channels, potassium channels, and voltage dependence of arterial smooth muscle tone. *Am J Physiol* **259**: C3–C18.

Peng H, Matchkov V, Ivarsen A, Aalkjaer C, Nilsson H (2001). Hypothesis for the initiation of vasomotion. *Circ Res* **88**: 810–815.

Philipson KD, Nicoll DA (2000). Sodium-calcium exchange: a molecular perspective. *Annu Rev Physiol* **62**: 111–133.

Poburko D, Kuo KH, Dai J, Lee CH, van Breemen C (2004). Organellar junctions promote targeted Ca2+ signaling in smooth muscle: why two membranes are better than one. *Trends Pharmacol Sci* **25**: 8–15.

Poburko D, Potter K, van Breemen E *et al*. (2006). Mitochondria buffer NCX-mediated Ca2+-entry and limit its diffusion into vascular smooth muscle cells. *Cell Calcium* **40**: 359–371.

Poburko D, Liao CH, Lemos VS, Lin E, Maruyama Y, Cole WC *et al*. (2007). Transient receptor potential channel 6-mediated, localized cytosolic [Na+] transients drive Na+/Ca2+ exchanger-mediated Ca2+ entry in purinergically stimulated aorta smooth muscle cells. *Circ Res* **101**: 1030–1038.

Putney JW Jr (1986). A model for receptor-regulated calcium entry. *Cell Calcium* **7**: 1–12.

Rahman A, Matchkov V, Nilsson H, Aalkjaer C (2005). Effects of cGMP on coordination of vascular smooth muscle cells of rat mesenteric small arteries. *J Vasc Res* **42**: 301–311.

Ratz PH, Berg KM (2006). 2-Aminoethoxydiphenyl borate inhibits KCl-induced vascular smooth muscle contraction. *Eur J Pharmacol* **541**: 177–183.

Rousseau E, Smith JS, Meissner G (1987). Ryanodine modifies conductance and gating behavior of single Ca2+ release channel. *Am J Physiol* **253**: C364–C368.

Rücker M, Strobel O, Vollmar B, Roesken F, Menger MD (2000). Vasomotion in critically perfused muscle protects adjacent tissues from capillary perfusion failure. *Am J Physiol Heart Circ Physiol* **279**: H550–H558.

Ruehlmann DO, Lee CH, Poburko D, van Breemen C (2000). Asynchronous Ca(2+) waves in intact venous smooth muscle. *Circ Res* **86**: E72–E79.

Shimamura K, Sekiguchi F, Sunano S (1999). Tension oscillation in arteries and its abnormality in hypertensive animals. *Clin Exp Pharmacol Physiol* **26**: 275–284.

Shirasawa Y, White RP, Robertson JT (1983). Mechanisms of the contractile effect induced by uridine 5-triphosphate in canine cerebral arteries. *Stroke* **14**: 347–355.

Sima B, Weir BK, Macdonald RL, Zhang H (1997). Extracellular nucleotide-induced [Ca2+]i elevation in rat basilar smooth muscle cells. *Stroke* **28**: 2053–2059.

Sobolevsky AI, Khodorov BI (1999). Blockade of NMDA channels in acutely isolated rat hippocampal neurons by the Na^+/Ca^{2+} exchange inhibitor KB-R7943. *Neuropharmacology* **38**: 1235–1242.

Streb H, Irvine RF, Berridge MJ, Schulz I (1983). Release of Ca2+ from a nonmitochondrial intracellular store in pancreatic acinar cells by inositol-1,4,5-trisphosphate. *Nature* **306**: 67–69.

Strobaek D, Olesen SP, Christophersen P, Dissing S (1996). P2-purinoceptor-mediated formation of inositol phosphates and intracellular Ca2+ transients in human coronary artery smooth muscle cells. *Br J Pharmacol* **118**: 1645–1652.

Toyoda K, Fujii K, Ibayashi S, Sadoshima S, Fujishima M (1996). Changes in arterioles, arteries, and local perfusion of the brain stem during hemorrhagic hypertension. *Am J Physiol* **270**: H1350–H1354.

Urquilla PR (1978). Prolonged contraction of isolated human and canine cerebral arteries induced by uridine 5′-triphosphate. *Stroke* **9**: 133–136.

Van Breemen C, Aaronson P, Loutzenhiser R (1978). Sodium-calcium interactions in mammalian smooth muscle. *Pharmacol Rev* **30**: 167–208.

Watano T, Kimura J, Morita T, Nakanishi H (1996). A novel antagonist, No. 7943, of the Na^+/Ca^{2+} exchange current in guinea-pig cardiac ventricular cells. *Br J Pharmacol* **119**: 555–563.

Weber LP, Van Lierop JE, Walsh MP (1999). Ca2+-independent phosphorylation of myosin in rat caudal artery and chicken gizzard myofilaments. *J Physiol* **516**: 805–824.

Wendt-Gallitelli MF, Voigt T, Isenberg G (1993). Microheterogeneity of subsarcolemmal sodium gradients. Electron probe microanalysis in guinea-pig ventricular myocytes. *J Physiol* **472**: 33–44.

Wilson DP, Sutherland C, Walsh MP (2002). Ca2+ activation of smooth muscle contraction: evidence for the involvement of calmodulin that is bound to the triton insoluble fraction even in the absence of Ca2+. *J Biol Chem* **277**: 2186–2192.

Xu L, Lai FA, Cohn A, Etter E, Guerrero A, Fay FS *et al*. (1994). Evidence for a Ca(2+)-gated ryanodine-sensitive Ca2+ release channel in visceral smooth muscle. *Proc Natl Acad Sci USA* **91**: 3294–3298.

Zacharia J, Zhang J, Wier WG (2007). Ca2+ signaling in mouse mesenteric small arteries: myogenic tone and adrenergic vasoconstriction. *Am J Physiol Heart Circ Physiol* **292**: H1523–H1532.